Available online at www.sciencedirect.com
ScienceDirect
Journal of the European Ceramic Society 30 (2010) 1489–1494
www.elsevier.com/locate/jeurceramsoc

Hot isostatic pressing of optically active Nd:YAG powders doped by a colloidal processing route

M. Suárez [a,c], A. Fernández [b], J.L. Menéndez [a], M. Nygren [c], R. Torrecillas [a], Z. Zhao [c,*]

[a] *Department of Nanostructured Materials, Centro de Investigación en Nanomateriales y Nanotecnología (CINN), Principado de Asturias – Consejo superior de Investigaciones Científicas (CSIC) – Universidad de Oviedo (UO), Parque Tecnológico de Asturias, 33428 Llanera (Asturias), Spain*
[b] *Fundación ITMA, Parque Tecnológico de Asturias, 33428 Llanera, Spain*
[c] *Department of Inorganic Chemistry, Arrhenius Laboratory, Stockholm University, SE-106 91 Stockholm, Sweden*

Received 20 March 2009; received in revised form 10 November 2009; accepted 27 November 2009
Available online 29 December 2009

Abstract

In this work, 1 at.% Nd doped Yttrium Aluminum Garnet $Y_3Al_5O_{12}$ (YAG) nano-sized powder prepared by colloidal route was investigated thoroughly concerning agglomeration control and preparation of transparent ceramic by post-HIP. Electrostatic and mechanical deagglomeration process followed by freeze-drying turned out to be an effective method to alleviate agglomeration, yielding a powder with a homogeneous particle size distribution around 100 nm. Transparent Nd:YAG ceramic samples have been successfully prepared by post-HIP without the aid of sintering additives. The optical properties varied markedly with the sintering and hot isostatic pressing conditions used. In-line transmittance values of 56% at 680 nm and close to 80% in the infrared region were recorded.

Keywords: Transparent ceramics; Nd:YAG; Colloidal route; Hot isostatic press

1. Introduction

Nd doped YAG laser material was first discovered by Geusic et al.[1] in 1964. Progress in crystal quality and optical properties of the produced materials have been improved with the use of fabrication techniques such as the Czochralski (Cz) method. In recent years, Nd:YAG (Nd:$Y_3Al_5O_{12}$) lasers have been applied with remarkable success to various industrial fields such as medical operation,[2,3] manufacturing for cutting and welding steel and various alloys, etc. Although, it would be desirable to increase the Nd concentration in the YAG matrix, as the laser power increases with increasing Nd content it is presently limited to 0.2–1.4 at.% in single crystals as a result of the segregation distribution coefficient.[4] Ikesue and Furusato[5] first demonstrated the possibility of fabricating transparent Nd:YAG ceramics with a sufficient quality for solid-state lasers with a reasonable efficiency. More recently, a number of studies have shown that transparent polycrystalline Nd:YAG ceramics are equivalent or even better than single crystals grown by the Czochralski method in terms of laser output power and efficiency.[6,7] Nowadays, polycrystalline Nd:YAG materials are highly preferred due to several key advantages over single crystals. For instance, the possibility of preparing large samples at low cost and an improved production rate opens up the door to mass production of this material. In addition, the possibility of increasing the neodymium doping concentration >4 at.% compared to melt-grown technologies makes it possible to miniaturize the laser materials and leads the way to new applications, such as single-mode microchip lasers.[8]

Concerning the methods for the fabrication of transparent YAG or Nd:YAG ceramics, either high temperature vacuum sintering[4,5] or post-hot isostatic press (post-HIP),[9,10] it is necessary to start from high purity and agglomeration-free powders. In addition, SiO_2, as an effective sintering additive, is often used to obtain transparent YAG or Nd:YAG ceramics.[4,5,7,11] Several techniques for the fabrication of rare earth oxides doped YAG ceramics have been recently employed[12–14] to overcome the difficulties, low sinterability, coarse particle size, bad dopant distribution and hard agglomerations, generally encountered in traditional solid-state reaction techniques. However, the agglomeration effect in the starting powders, which is essential to eliminate as much as possible pores in transparent ceramics, is not investigated systematically. Very recently, the agglomeration

* Corresponding author. Tel.: +46 8 162417; fax: +46 8 152187.
E-mail address: zhe.zhao@mmk.su.se (Z. Zhao).

0955-2219/$ – see front matter © 2009 Elsevier Ltd. All rights reserved.
doi:10.1016/j.jeurceramsoc.2009.12.006

effect in transparent Y_2O_3[15] and Nd:YAG[16,17] were investigated carefully. The additional freeze-drying process with precursor powders was demonstrated to be effective to reduce the agglomeration in the calcined powders and led to improved optical properties. It is believed that freeze-drying with precursor led to better sinterability. But there is no study available in literature to investigate the effect of freeze-drying on the control of agglomeration state in final synthesized or commercial powders and thus the influence on sintering and optical properties.

In this paper, we firstly show the effectiveness of agglomeration control by electrostatic dispersion and milling process with the highly agglomerated Nd:YAG powder prepared by a colloidal doping route from synthesized YAG; secondly, we will demonstrate that proper sintering parameter selection for post-HIP can lead to success of transparent Nd:YAG ceramic without SiO_2 presence.

2. Experimental

Nano-sized Yttrium Aluminum Garnet (YAG) powder with average grain size of 100 nm was first obtained by using a reverse-strike precipitation method using $AlCl_3{\cdot}9H_2O$ (98%), $YCl_3{\cdot}6H_2O$ (99.9%) with a molar ratio of 5:3 and ammonium hydroxide solution (28% in water) as reactants. Keeping a constant pH value during the process is critical for the control of chemical homogeneity within the particles.[18] After 24 h of aging, a gelatinous precipitate was obtained. Then, solvent was removed by centrifugation steps and subsequently the amorphous gel was dried in an oven. After that, a colloidal method was implemented[19] to dope pure YAG with Nd. The doping was carried out under argon atmosphere by dissolving the appropriate quantity of neodimium methoxiethoxide in anhydrous ethanol (99.97%) which was then added dropwise to the YAG/ethanol slurry to get Nd:YAG powder with 1 at.% Nd. The slurry was first dried under magnetic stirring between 60 and 70 °C and subsequently in air at 120 °C in order to eliminate most alcohol. The dried powders were crushed in a high purity alumina mortar to remove the agglomerates resulting from the drying process and sieved using a 63 μm mesh. The powders were calcined at 800 °C for 2 h in air in order to remove organic residuals in accordance with thermogravimetric analysis (TG-DSC, Instruments Model SDT 2960) conducted in air atmosphere using a heating rate of 5 °C/min up to 900 °C. The powder produced by the above procedure was hereafter named as as-prepared powder. The zeta-potential and particle size measurement for as-prepared Nd:YAG powder was taken by Malvern Nanosizer Nano-ZS.

In order to destroy the agglomerates in the as prepared powder, freeze-drying was implemented. Nd:YAG slurries with solid contents of 40 wt% were prepared in deionized water at pH 2 and milled with zirconia beads for 6 h in a planetary milling machine (Retsch PM100). Frozen droplets were formed by spraying slurry in to the liquid nitrogen through a nozzle. Then, the powder was dried in freeze-dryer (Hetosicc Model) for three days at −50 °C and 0.5 mbar pressure. The powder produced by this process was hereafter named as freeze-dried powder. The agglomeration state and particle size of the powders was observed using a high-resolution scanning electron microscope, SEM (JEOL JSM-7000F).

A dilatometric study (Dilatometer DIL 402C, Netzsch) of the sintering behavior was carried out up to 1800 °C at a heating rate of 5 °C/min in air. The prepared powders were cold isostatically pressed (CIP) at 200 MPa prior to sintering. Finally the samples sintered at selected temperatures (1650 and 1680 °C) were further HIPed to get transparent ceramics. The post-HIP treatment was done with argon as media and a pressure of 200 MPa. The density of the samples was measured by the Archimedes method using deionized water as the immersion liquid. A theoretical density of 4.55 g cm^{-3} was used for relative density calculation.[20] The microstructures of the prepared samples were studied by SEM (DSM 950 Zeiss model). The SEM samples were mechanically polished using diamond sprays down to 1 μm and thermally etched at 1400 °C for 1 h. The average final grain size was measured using the intercept analysis method developed by Smith and Guttman,[21] using 1.56 as the stereological correction factor. The transmission spectrum was recorded on VIS (AvaSpec-2048-2) and IR (Nicolet Magna IR-560®) equipments. The emission spectrum was recorded on a Bruker MSL-400 system.

3. Results and discussion

The morphology of the freeze-dried and as-prepared Nd:YAG powders, are shown in Fig. 1(a) and (b), respectively. Fig. 1(a) reveals that the freeze-dried Nd:YAG powders are well dispersed

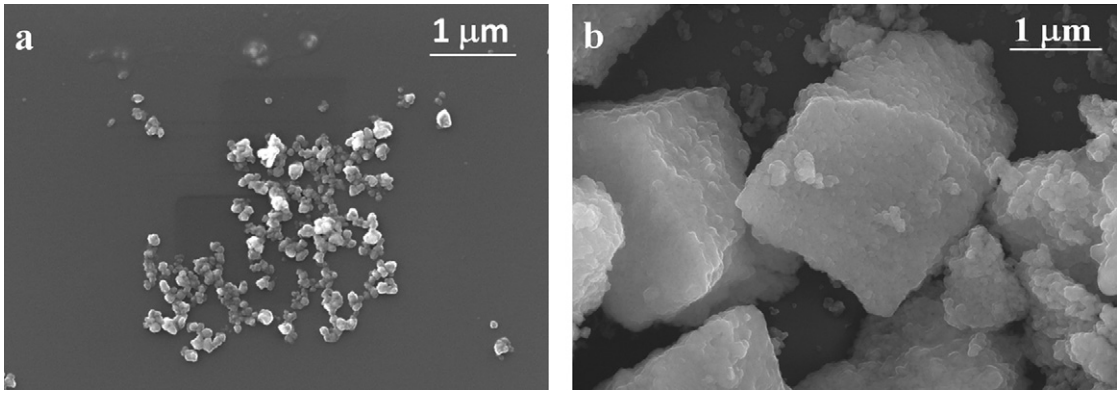

Fig. 1. Morphology of the Nd:YAG powders (a) freeze-dried and (b) as-prepared.

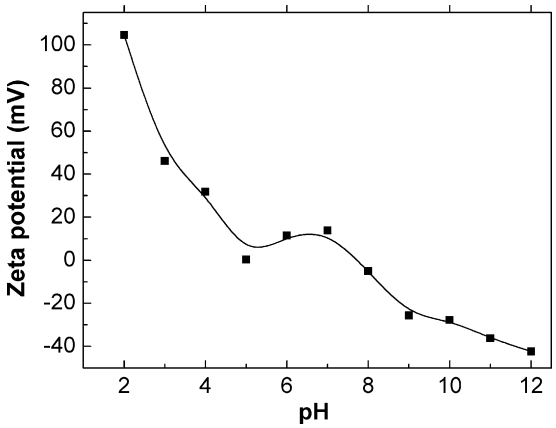

Fig. 2. Variation of zeta-potential with pH for Nd:YAG powders.

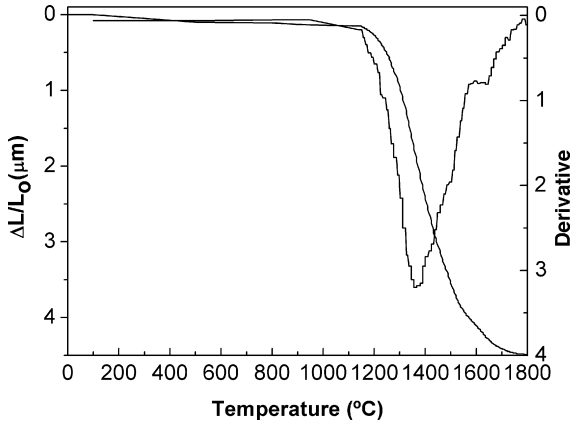

Fig. 3. Dilatometry curve and derivate for a cold pressed green body of Nd:YAG powder. The heating rate was 5 °C/min.

with an average particle size around 100 nm without indication of agglomeration. On the other hand, the as-prepared powders shown in Fig. 1(b) reveal the presence of large agglomerated particles with size around 1–2 μm which are always consisted of smaller crystallite with size about 100 nm. Milling has been widely used as the most common technique to reduce the average particle size by either crystal cleavage or particle detachment. But the strong tendency to agglomerate in nano-sized particles always makes such simple milling process less effective. As indicated in Fig. 2, highest zeta-potential of 104.5 mV was obtained at pH 2. In this case, the repulsive electrostatic force between 100 nm Nd:YAG crystallites can ensure a perfect dispersion in water if the agglomerates can be broken down by the mechanical force in planetary milling. In such a sequence, the following freeze-drying can lead to an agglomeration-free powder through a gentle water evaporation process. Without doubt, we may conclude that an electrostatic and mechanical deagglomeration process followed by freeze-drying is an effective method to avoid agglomerates, yielding a material with a homogeneous particle size distribution.

To further elucidate the effect of deagglomeration on sintering performance, the as-prepared and freeze-dried powders were sintered at 1650 °C for 4 h with a constant heating rate 5 °C/min. The freeze-dried powder can reach a density of 92.0%, meanwhile the as-prepared powder only get 76.0%, which is far below the density limit (92–93%) for a non-encapsulating post-HIP treatment. Only the freeze-dried powder can be used for further post-HIP treatment to get transparent ceramics. Such a dramatic change in density again illustrated the importance of proper powder deagglomeration treatment, especially for pressureless sintering.

For the selection of pre-sintering and HIP temperature, a dilatometric study with the freeze-dried powder was carried out in air up to 1800 °C with constant heating rate of 5 °C/min. The linear shrinkage curve is shown in Fig. 3. It can be seen that the material starts shrinkage around 1140 °C and stops around 1750 °C, while the maximum shrinkage rate is reached at ∼1350 °C. So the temperatures of 1650 and 1680 °C were chosen for the pre-sintering experiments as these temperatures ought to yield compacts with closed pore structure and density between 92 and 96%, which is the major premise for a non-encapsulating post-HIP. It has been reported that a minimum relative density of 94–95% is required for a good performance in the following post-HIP procedure in order to get highly transparent Al_2O_3 ceramics.[22] For the purpose of depressing grain growth as much as possible to improve the mechanical strength and thermal shock resistance, which are highly recommended by the recent solid-state laser engineering, two HIP treatment temperature of 1650 and 1700 °C were selected.

In Table 1, the sintering parameters and densities for all four post-HIPed samples (A1–A4) are listed. Relative densities of 92 and 97% were successfully obtained after pre-sintering in air at 1650 and 1680 °C. Post-HIP generally improves the densities for all four samples. However, it was found pre-sintered samples with a relatively high density of 97% (A3 and A4) got a worse density compared to the samples with lower pre-sintering density of 92% (A1 and A2). The samples pre-sintered at 1650 °C (A1 and A2) can reach a density of 99.7% by the HIP at both 1650 and 1700 °C. By contrary, for samples pre-sintered at 1680 °C, higher HIP temperature of 1700 °C (A4) even led to a slight reduction in the final density compared with HIP at 1650 °C. All these results suggest that the initial pre-sintering density is

Table 1
Sintering parameters and densities for post-HIP samples.

Specimen number	Pre-sintering temperature (°C)	Density (%)	HIP temperature (°C)	Density (%)
A1	1650	91.9 ± 0.5	1650	99.7 ± 0.3
A2	1650	91.9 ± 0.5	1700	99.7 ± 0.3
A3	1680	96.5 ± 0.5	1650	99.0 ± 0.5
A4	1680	96.5 ± 0.5	1700	98.8 ± 0.5

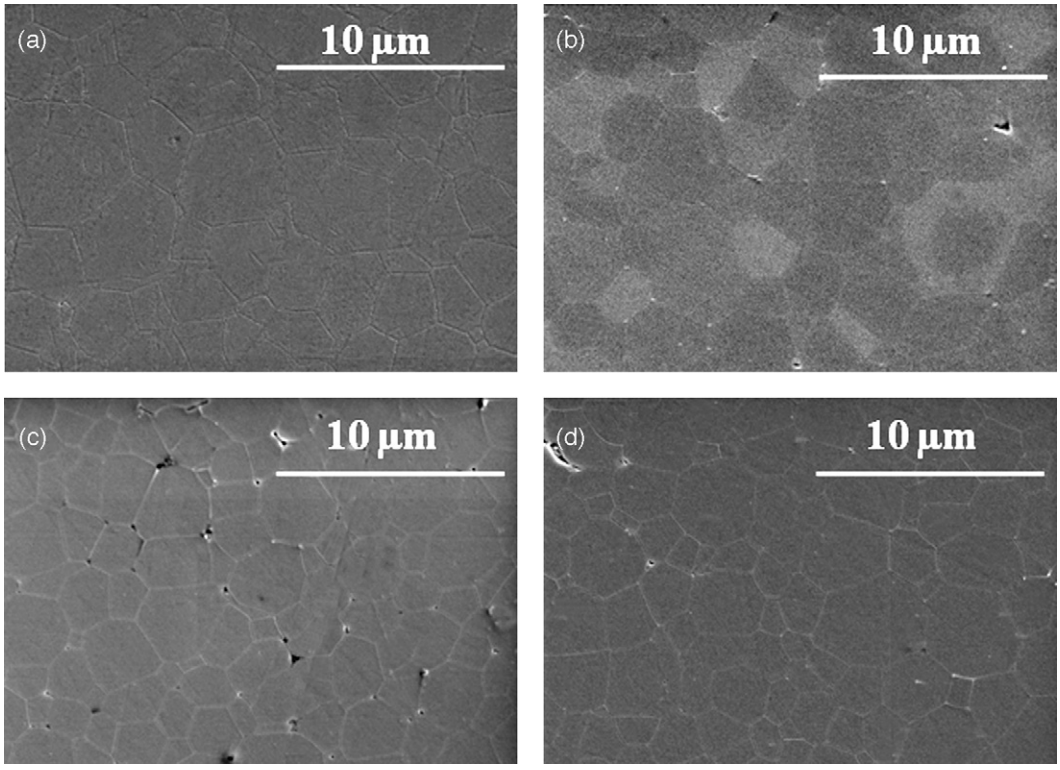

Fig. 4. SEM micrographs of specimens A1 (a) and A2 (b), A3 (c) and A4 (d).

not the only factor in determining the final density after HIP process.

The SEM micrographs of the samples A1–A4 are shown in Fig. 4. It shows that the microstructures of samples with the same pre-sintering temperature are very similar in terms of grain size and pores structure. A1 and A2 both show a pore-free structure and the average grain sizes are 7.0 ± 2.0 and 8.0 ± 1.5 μm, respectively. Meanwhile, A3 and A4 both show residual pores at triple junctions and the average grain sizes are 5.0 ± 1.5 and 5.0 ± 1.5 μm. During HIP process, the main driving force for further densification is mechanical stress realized by a pressurizing gas (Ar). This should generally facilitate the removal of residual pores in the pre-sintered ceramic compacts. In this case, the potential densification mechanism of creep at high temperature should be considered. For this, lower relative density and higher temperature will be beneficial for the densification due to the enhanced deformation ability. It is rational to suppose that the small difference between pre-sintering and HIP temperature for A3 and A4 cannot introduce more thermally induced densification. A density of 97% might be too high to realize effective densification through a deformation mechanism. The homogeneous grain size and pore size distribution in A3 and A4 indicate that the abnormal grain growth or poor pore structure should be excluded as the reason leading to worse sintering behavior. A similar phenomenon has been reported in the transparent $MgAl_2O_4$ ceramics prepared by hot-pressing plus post-HIP.[23] Lower hot-pressing temperature always leads to better light transmittance in visible wavelength range, which is sensitive to porosity and pore size. But the further improvement in density by further increasing HIP temperature cannot be simply excluded, even for A3 and A4. Actually, once effective densification mechanism can be activated, in the case of A1 and A2, the increase of HIP temperature definitely results in better optical properties even the density data shows no difference.

The in-line transmittance spectra (400 nm–6 μm) for the samples A1–A4 are given in Fig. 5. The samples A3 and A4 show low values of transmittance due to the presence of residual porosity, making it impossible to characterize them in the visible range. The main differences between samples A1 and A2 are found in the visible range. Sample A1 shows a dramatic decrease of the in-line transmittance in the visible range below 1 μm. This can be further confirmed by the outlook of samples shown in Fig. 6, sample A1 (Fig. 5(a)) clearly is less transparent than A2 (Fig. 5(b)). But this difference cannot be simply explained in

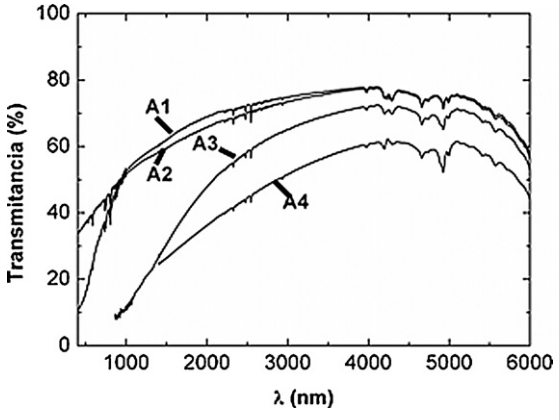

Fig. 5. The real in-line optical transmittance spectra for samples A1–A4.

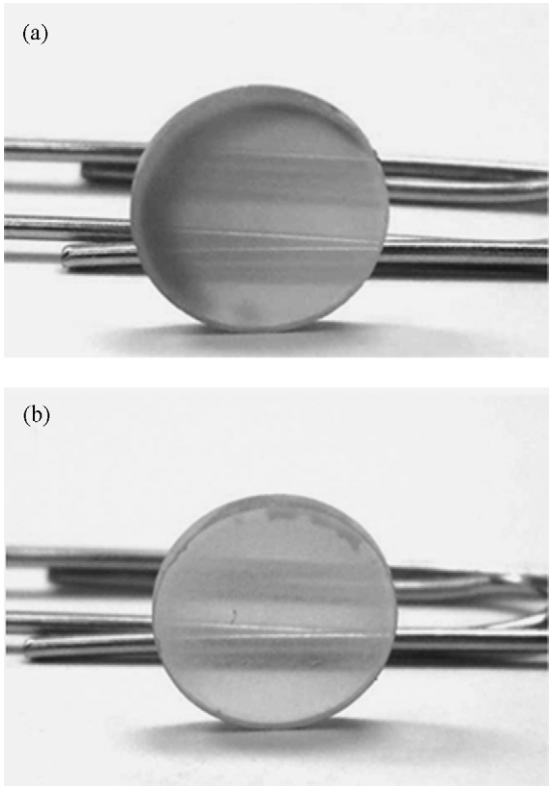

Fig. 6. Photographs showing the appearance of Nd:YAG transparent ceramics: specimen A1 (a) and A2 (b).

terms of density or grain size. However, as we mentioned above that the increase of HIP temperature can potentially further remove the minor amount defects which cannot be detected by a simple water immersion density measurement. Also, sample A2 presents a high intensity absorption line at 588 nm which can be assigned to the distortion of neodymium sites in the material.[24] This result indicates that Nd^{3+} ions in sample A1, HIPed at 1650 °C have not entered the YAG crystal lattice, whereas Nd^{3+} ions in sample A2, HIPed at 1700 °C have already entered the YAG crystal lattice. The other strong bands, located between 500 and 1000 nm, can be ascribed to the absorption due to transitions of the Nd^{3+} ions.[24] The emission spectra of samples A1 and A2 are shown in Fig. 7. Under the excitation of 532 nm diode laser, both samples show the same emission lines and their spectra are identical to that of a YAG single crystal doped with 1 at.% of Nd. The peaks belong to the transition between the excited $^4F_{3/2}$ to lower energy, $^4I_{11/2}$ levels. The spectra show that the emission of YAG samples doped with 1 at.% Nd is centered on 1064.2 nm.

The highest in-line transmittance, for a thickness of 0.8 mm, 56% at 680 nm and nearly 80% in the infrared range is achieved in A2. This is similar to the transparent Nd:YAG ceramic by vacuum sintering while with SiO_2 as sintering additive.[25] Li et al.,[26] have demonstrated that transparent YAG can be prepared from nanocrystalline powder by vacuum sintering without SiO_2 presence, but there is no transmittance data available. Here, the success of transparent Nd:YAG ceramic by post-HIP without SiO_2 as sintering additive further extend the possibilities of

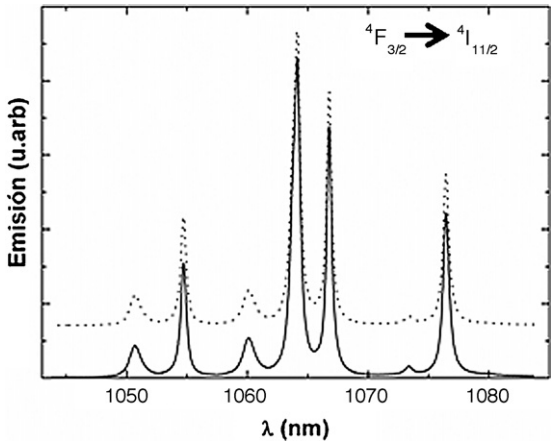

Fig. 7. Optical emission ($^4F_{3/2} \rightarrow {}^4I_{11/2}$ transition) spectra of A1 (solid line) and A2 (doted line).

improving the quality of Nd:YAG laser ceramics, where SiO_2 might introduce defects bad for laser performance.

4. Conclusions

In conclusion, Nd:YAG powders with an average size about 100 nm have been prepared following a colloidal doping route. Electrostatic and mechanical deagglomeration process followed by freeze-drying turned out to be an effective method to avoid agglomerates, yielding a material with a homogeneous particle size distribution. Dense Nd:YAG ceramic samples with a high degree of transparency have been successfully prepared by conventional sintering and post-HIP treatment without use of SiO_2 as sintering additive. A potential densification mechanism of creep at high temperature has been considered, showing that relatively lower density before HIP and higher HIP treatment temperature will be beneficial for the densification due to the enhanced densification. A high in-line transmittance value, up to 56% at 680 nm and close to 80% in the infrared range, for 0.8 mm thick samples were obtained without SiO_2 as sintering additive. Finally, it has been found that the emission spectra of samples A1 and A2 under the excitation of a 532 nm diode laser are identical to that of a Nd:YAG single crystal with 1 at.% Nd.

Acknowledgments

The authors acknowledge the Spanish Ministry of Education and Science and UE for funding through projects MAT2006-01783 and NMP3-CT-2005-515784, respectively. M. Suárez acknowledges CSIC for an I3P fellowship. Authors would like to thank Dr. Guillaume Bernard-Granger in Saint-Gobain for the help with HIP experiments.

References

1. Geusic JE, Marcos HM, Van Uitert LG. Laser oscillations in Nd-doped yttrium aluminium, yttrium gallium and gadolinium garnets. *Appl Phys Lett* 1964;**4**:182–4.
2. Walfisch S, Mnitentag H, Baruchin AM, SAGI A. Nd:YAG and CO_2 lasers for the treatment of pilonidal sinuses: advantages over traditional techniques. *Med Laser Appl* 2004;**19**:155–9.

3. Savastru D, Miclos S, Cotîrlan C, Ristici E, Mustata M, Mogîldea M, et al. Nd:YAG Laser system for ophthalmology: Biolaser-1. *J Optoelec Adv Mater* 2004;**6**:497–502.
4. Lee S-G, Kochawattana S, Messing GL, Dumm JQ, Quarles G, Castillo V. Solid-state reactive sintering of transparent polycrytalline Nd:YAG ceramics. *J Am Ceram Soc* 2006;**89**:1945–50.
5. Ikesue A, Furusato I. Fabrication of polycrystalline transparent YAG ceramics by a solid-state reaction method. *J Am Ceram Soc* 1995;**78**:225–8.
6. Lu J, Ueda K-I, Yagi H, Yanagitani T, Akiyama Y, Kaminskii AA. Neodymium doped yttrium aluminum garnet ($Y_3Al_5O_{12}$) monocrystalline ceramics—a new generation of solid state laser and optical materials. *J Alloys Compd* 2002;**341**:220–5.
7. Rabinovitch Y, Tétard D, Faucher MD, Pham-Thi M. Transparent polycrystalline neodymium doped YAG: synthesis parameters, laser efficiency. *Opt Mater* 2003;**24**:345–51.
8. Sulc J, Jelínková H, Nejezchleb K, Skoda V. Nd:YAG/V:YAG microchip laser operating at 1338 nm. *Laser Phys Lett* 2005;**2**:519–24.
9. Ikesue A, Kamata K. Microstructure and optical properties of hot isostatically pressed Nd:YAG ceramics. *J Am Ceram Soc* 1996;**79**:1927–33.
10. Lee S-H, Kupp ER, Stevenson AJ, Anderson JM, Messing GL, Li X, et al. Hot isostatic pressing of transparent Nd:YAG ceramics. *J Am Ceram Soc* 2009;**92**:1456–63.
11. Ikesue A. Polycrystalline Nd:YAG ceramics lasers. *Opt Mater* 2002;**19**:183–7.
12. Li X, Liu H, Wang J, Cui H, Zhang X, Han F. Preparation of YAG:Nd nano-sized powder by co-precipitation method. *Mater Sci Technol A* 2004;**379**:347–50.
13. Ruan S-K, Zhou J-G, Zhong A-M, Duan J-F, Yang X-B, Su M-Z. Synthesis of $Y_3Al_5O_{12}$: Eu^{3+} phosphor by sol–gel method and its luminescence behavior. *J Alloys Compd* 1998;**257–277**:72–5.
14. Li J, Pan Y, Qiu F, Wu Y, Guo J. Nanostructured Nd:YAG powders via gel combustion: the influence of citrate-to-nitrate ratio. *Ceram Int* 2008;**34**:141–9.
15. Mouzon J, Lindbäck T, Oden M. Influence of agglomeration on the transparency of yttria ceramics. *J Am Ceram Soc* 2008;**91**:3380–7.
16. Rabinovitch Y, Bogicevic C, Karolak F, Tetard D, Dammak H. Freeze-dried nanometric neodymium-doped YAG powders for transparent ceramics. *J Mater Process Technol* 2008;**199**:314–20.
17. Gong H, Tang D-Y, Huang H, Ma J. Agglomeration control of Nd:YAG nanoparticles via freeze drying for transparent Nd:YAG ceramics. *J Am Ceram Soc* 2009;**92**:812–7.
18. Palmero P, Esnouf C, Montanaro L, Fantozzi G. Influence of the co-precipitation temperature on phase evolution in yttrium–aluminum oxide materials. *J Eur Ceram Soc* 2005;**25**:1565–73.
19. Schehl M, Díaz LA, Torrecillas R. Alumina nanocomposites from powder–alkoxide mixtures. *Acta Mater* 2002;**50**:1125–39.
20. Chaim R, Marder-Jaeckel R, Shen JZ. Transparent YAG ceramics by surface softening of nanoparticles in spark plasma sintering. *Mater Sci Eng A* 2006;**429**:74–8.
21. Smith CS, Guttman L. Measurement of internal boundaries in three-dimensional structures by random sectioning. *Trans AIME* 1953;**197**:81–7.
22. Krell A, Blank P, Ma H, Hutzler T. Transparent sintered corundum with high hardness and strength. *J Am Ceram Soc* 2003;**86**:12–8.
23. Gilde G, Patel P, Patterson P, Blodgett D, Duncan D, Hahn D. Evaluation of hot pressing and hot isostatic pressing parameters on the optical properties of spinel. *J Am Ceram Soc* 2005;**88**:2747–51.
24. Barnakow YA, Veal I, Kabato Z, Zhu G, Bahoura M, Noginov MA. Simple route to Nd:YAG transparent ceramics. In: *SPIE, Defense and Security Symposium*. 2006.
25. Li X, Li Q, Wang JY, Yang SL, Liu H. Synthesis of Nd^{3+} doped nanocrystalline yttrium aluminum garnet (YAG) powders leading to transparent ceramic. *Opt Mater* 2007;**29**:528–31.
26. Li JG, Ikegami T, Lee JH, Mori T. Low-temperature fabrication of transparent yttrium aluminum garnet (YAG) ceramics without additives. *J Am Ceram Soc* 2000;**83**:961–3.